

Causal Mechanisms of Dyslexia Via Connectogram Modeling of Phase Synchrony

I. Rodríguez-Rodríguez^{1,2}, A. Ortiz^{1,2}, M.A. Formoso^{1,2}, N.J. Gallego-Molina^{1,2}, and J.L. Luque³

¹ Communications Engineering Department
University of Málaga. 29004 Málaga, Spain

² Department of Developmental and Educational Psychology, University of Málaga.29004 Málaga, Spain

³ Andalusian Data Science and Computational Intelligence Institute (DaSCI)

Abstract. This paper introduces connectogram modeling of electroencephalography (EEG) signals as a novel approach to represent causal relationships and information flow between different brain regions. Connectograms are graphical representations that map the connectivity between neural nodes or EEG channels through lines and arrows of varying thickness and directionality. Here, inter-channel phase connectivity patterns were analyzed by computing Granger causality to quantify the magnitude and direction of causal effects. The resulting weighted, directed connectograms displayed differences in functional integration between individuals with developmental dyslexia versus fluent readers when processing 4.8 Hz amplitude-modulated noise, designed to elicit speech encoding mechanisms. Machine learning classification was subsequently implemented to distinguish participant groups based on characteristic connectivity fingerprints. The methodology integrates signal filtering, instantaneous phase analysis via Hilbert transform, Granger causality computation between all channel pairs, automated feature selection using novel mutual information filtering, construction of directed weighted connectograms, and Gradient Boosting classification. Classification analysis successfully discriminates connectivity patterns, directly implicating theta and gamma bands (AUC 0.929 and 0.911, respectively) resulting from rhythmic auditory stimulation. Results demonstrated altered cross-regional theta and gamma band oscillatory connectivity in dyslexia during foundational auditory processing, providing perspectives on multisensory and temporal encoding inefficiencies underlying language difficulties.

Keywords: EEG · connectograms · dyslexia · Granger causality · Hilbert · Gradient Boosting

1 Introduction

Developmental dyslexia (DD), affecting 5-12% of learners [14], is a prevalent learning disability causing reading and writing difficulties. However, traditional diagnosis based on behavioral tests can be subjective and vulnerable to external factors. Hence, objective techniques are imperative for accurate early detection, based on the latest techniques [5]. Connectivity analysis of brain signals is promising for revealing DD biomarkers.

Specifically, electroencephalography (EEG) enables noninvasive measurement of cortical activity with high temporal resolution. EEG studies have identified connectivity patterns related to neurological disorders and language faculties [18], elucidating coordination between regions during cognitive tasks [19]. Connectivity modeling can reveal directional relationships [23].

The theory proposes that phase synchronization deficits, impeding phonological development [6], may arise from atypical low-frequency neural speech encoding in DD. DD learner EEG studies have evidenced differential entrainment between frequency bands when processing speech [12]. Various methods have explored EEG spectral, statistical, and graphical features to analyze connectivity [4]. Further insight may arise by tools like Granger causality to probe oscillatory coordination [9].

We generate connectivity models by examining inter-channel phase Granger causality [7] relationships under prosodic auditory stimuli. Adopting a novel approach, directed weighted connectograms represent causal links between EEG channels. While connectograms effectively depict complex connectivity patterns from neuroimaging, we extend them to EEG classification through machine learning, addressing EEG signal intricacies. Specifically, we implement Gradient Boosting with the novel Mutually Informed Correlation Coefficient (MICC) filter for feature selection [8]. We seek to demonstrate distinct network connectivity fingerprints in DD learners during foundational auditory processing.

Our methodology trains models on an age-matched dataset [13] of DD and control learners. Preprocessing removes artifacts before bandpass filtering EEG channels into five frequency bands. Then, the Hilbert transform extracts phase components to compute Granger causality between all channel pairs, quantifying causal relationships to construct weighted directed connectograms displaying interplay polarity and strength. We classify groups using feature sets filtered for mutual information with DD labels and low inter-feature correlation.

This work introduces connectogram modeling of causal EEG dynamics for studying developmental disorders. By integrating signal processing, connectivity mapping, feature selection, and classification, the pipeline delivers enhanced EEG analytics. The approach expands the current understanding of brain network interactions in DD while demonstrating the feasibility of accurate automated screening. Findings could inform diagnostics and interventions for complex neurodevelopmental conditions.

2 Material and methods

2.1 Data acquisition

The EEG dataset was collected from 48 Spanish-speaking children aged 88-100 months, including 32 proficient readers and 16 children formally diagnosed with DD. Participants had normal or corrected vision without auditory issues. Prior to the experiment, guardians were informed and provided consent. The children were exposed to 15 minutes of white noise auditory stimulus modulated at 4.8Hz to elicit foundational auditory processing patterns, informed by expertise on prosodic-syllabic frequencies in speech. EEG signals were captured using 32 electrode actiCAP per the 10-20 system, sampled at 500Hz.

2.2 Preprocessing

The EEG signals underwent preprocessing to remove artifacts, including using independent component analysis to eliminate eye-blinking artifacts based on EOG channel observations and discarding segments with movement or impedance variations. Channels were then referenced to Cz. Next, signals passed through finite impulse response bandpass filters to obtain information within delta (1.5-4 Hz), theta (4-8 Hz), alpha (8-13 Hz), beta (13-30 Hz), and gamma (30-80 Hz) EEG bands without phase distortion that would occur with other filters. The two-way zero phase lag filtering compensates for phase lags. With the 80 Hz low-pass filtering, a 50 Hz notch filter was also applied during preprocessing to remove that frequency component.

2.3 Hilbert Transform

A Hilbert Transform (HT) can convert an actual signal into an analytic signal, a complex valued time series without negative frequency components. Performing a HT facilitates the computation of the time-varying amplitude, phase, and frequency of the analytic signal, termed the instantaneous amplitude, phase, and frequency.

The HT is mathematically defined for a signal $x(t)$, as shown in equation (1). By combining the original signal $x(t)$ with its HT, the analytic signal $z(t)$ can be obtained for signal $x(t)$ as shown in equation (2).

$$\mathcal{H}[x(t)] = \frac{1}{\pi} \int_{-\infty}^{+\infty} \frac{x(\tau)}{t - \tau} d\tau \quad (1)$$

$$z_i(t) = x_i(t) + j\mathcal{H}x_i(t) = a(t)e^{j\phi(t)} \quad (2)$$

From the analytic signal $z(t)$, it is straightforward to compute the instantaneous, unwrapped phase $\phi(t)$ can be obtained using the arctangent function on $z(t)$ as shown in equation (3).

$$\phi(t) = \tan^{-1} \frac{\text{im}(z_i(t))}{\text{re}(z_i(t))} \quad (3)$$

Applying this HT provides the phase value for each time point. So, the phase component $\phi(t)$ facilitates a more nuanced analysis of oscillatory brain activities.

2.4 Granger Causality

Granger causality, first introduced by economist Clive Granger [7], is a statistical approach frequently used to assess causal interactions between continuous-valued time series. It is grounded in the premise that while the past and present may cause the future, the future cannot retroactively impact the past. More specifically, if x_t and y_t denote two stationary time series, then x_t is said to Granger-cause y_t if incorporating past values of x_t provides significantly improved prediction of future y_t compared to only using auto-regression based on past y_t values. Mathematically, let x_{t-k} and y_{t-k} represent the past k values of x_t and y_t , respectively. Granger causality can then be examined via the following two auto-regressive models:

$$\hat{y}_{t1} = \sum_{k=1}^l a_k y_{t-k} + \varepsilon_t \quad (4)$$

$$\hat{y}_{t2} = \sum_{k=1}^l a_k y_{t-k} + \sum_{k=1}^w b_k x_{t-k} + \eta_t \quad (5)$$

Here ε_t , η_t are white noise prediction errors, while a_k and b_k are least squares regression coefficient vectors fitted over l past x values and w past y values, respectively. Since real-world time series are finite, w is chosen significantly below the series length, optimized via the Akaike Information Criterion (AIC) [1]. If the F-test applied to (4) and (5) produces a p-value indicating significantly improved regression performance for (5), we conclude that x_t Granger causes y_t .

2.5 Feature Selection

The Mutually Informed Correlation Coefficient (MICC) [8] is a novel filter-based feature selection method to efficiently extract the most discriminative and relevant features from high-dimensional vectors for pattern classification problems. MICC scores each feature by combining mutual information (MI) and Pearson's correlation coefficient (PCC). MI measures the dependence between a feature and the class label. A higher MI indicates a more informative feature for classification. PCC quantifies the correlation between features. Higher PCC implies greater redundancy. The MICC score in equation (8) balances these components. $MI(i)$ calculates mutual information between feature i and class label C . $PCC(i, j)$ sums correlations of feature i with all other features. The parameter controls this trade-off. Features are ranked by MICC score for selection.

$$PCC(x, y) = \frac{1}{(n-1)} \sum_{i=1}^n \frac{(x_i - \bar{x})(y_i - \bar{y})}{(s_x s_y)} \quad (6)$$

$$MI(A; B) = \sum_x \sum_y p(a, b) \log \frac{p(a, b)}{p(a)p(b)} \quad (7)$$

$$score(i) = \alpha \times MI(i) - (1 - \alpha) \times \sum_{j=1}^{dim} PCC(i, j) \quad (8)$$

As equation (6) shows, PCC determines a linear relationship between features x and y using means, standard deviations, and covariance. It ranges from -1 to 1, with 0 indicating no correlation. MI in equation (7) computes dependence between variables A and B using joint and marginal distributions. Higher MI values denote greater dependence.

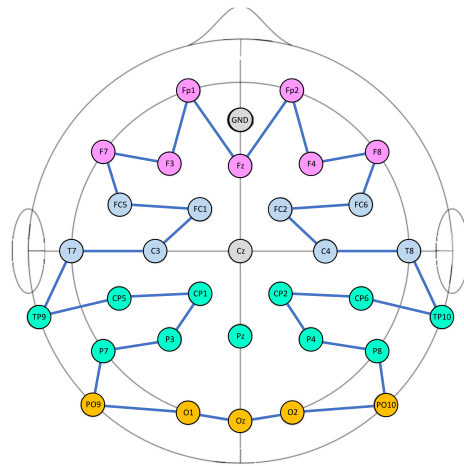


Fig. 1: Connectogram from the 10-20 system, 32 electrodes

2.6 Connectograms

Connectograms are invaluable neuroscientific tools to represent intricate brain connectivity patterns. Initially developed for magnetic resonance imaging (MRI), connectograms now also model electroencephalography (EEG) dynamics as networks of interconnected nodes and pathways mirroring neural connections and activities [3]. The spectrograms reflect a formation of 32 electrodes following the 10-20 system (Figure 1).

Incorporating directionality and weighting further enhances EEG connectograms. Directed graphs account for asymmetric causality between nodes, unlike symmetric correlations. If electrode A influences B more than vice versa, connectograms can reveal such directional brain activity drivers [7]. Weighting via Granger causality numerically signifies causal influence strength between EEG channels. Higher weights (lower Granger values) indicate greater certainty of one channel driving another, while lower weights suggest more ambiguous effects.

2.7 Machine Learning classification

Ensemble methods amalgamate multiple diverse models via weighted majority voting to enhance prediction accuracy and stability beyond individual techniques. The critical concept involves synthesizing superior joint forecasts from the discrete outputs of component models.

Boosting initializes by weighting all training examples equally. However, weights are iteratively updated based on prediction accuracy from previous iterations. Incorrectly classified cases receive amplified emphasis in subsequent models. Meanwhile, examples already predicted precisely endure attenuated significance. Thus, ensembles systematically stress overlooked nuances that no single model captures completely.

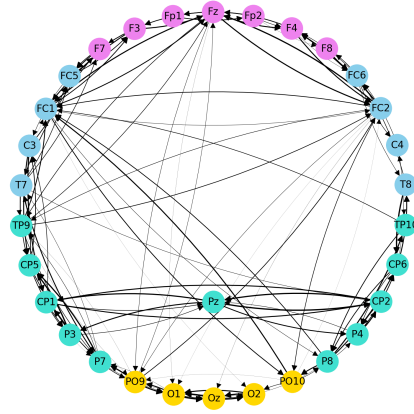


Fig. 2: Causality in control group, theta

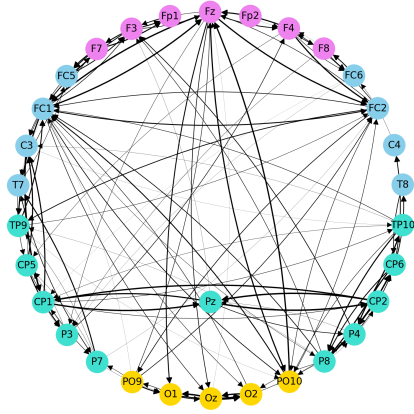


Fig. 3: Causality in dyslexic group, theta

Gradient Boosting minimizes deviation or error metrics through iterative forward stagewise fitting of regression trees onto residuals. For binary classification, each iteration only fits one tree. By constructing additive models sequentially, Gradient Boosting concentrates new trees on minimizing the loss function gradient unexplained by previous iterations. The Mutually Informed Correlation Coefficient filter promises to improve performance while reducing complexity.

Extensive cross-validation across parameter grids optimizes tuning. Owing to ensemble diversity unlocking intricate patterns combined with exhaustive nonlinear residual fitting, Gradient Boosting excels at delivering accurate predictions across small, complex data where individual models falter.

3 Results

The direct preliminary representation of the Granger matrices in the control and dyslexia groups offers, at first glance, greater causal connectivity in the dyslexia group, as noted in [17]. Figure 3 (Connectogram of causality in dyslexic group) indicates this greater connection exemplified for the theta band than the control group (Figure 2).

Features scores (FS) have been depicted in a bar graph (Figure 4) and the respective connectogram (Figure 5), and show differentiated functional connectivity between occipital and frontal brain regions (Oz-F8, O2-Fp1) in individuals with dyslexia when presented with a 4.8Hz stimulus corresponding to the theta band. The occipital regions are involved in visual processing, while the frontal regions underpin executive functions like attention. As theta oscillations facilitate coordination between memory, attention, and perception, altered occipital-frontal theta synchronization likely contributes to difficulties with sensory context encoding and semantic processing in dyslexia [21].

Additionally, more significant frontal cortical activity is observed in people with dyslexia across frequency bands, suggesting compensation for deficiencies in early

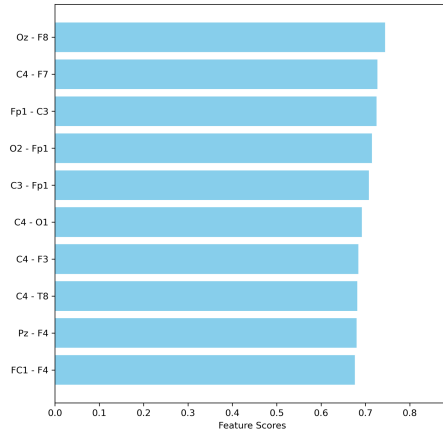


Fig. 4: Bar graph of FS, theta

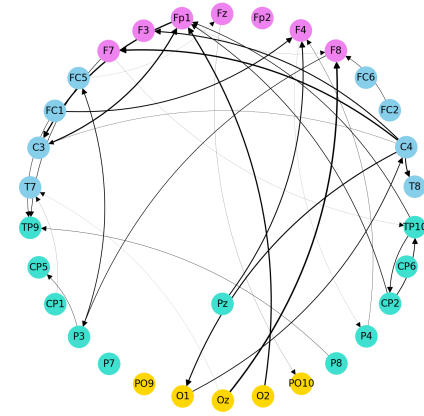


Fig. 5: Connectogram of FS, theta

visual processing stages (C4-F7, Fp1-C3) [15]. However, reduced auditory network connectivity is seen in dyslexics' right hemispheres, specifically in the theta band. This highlights potential difficulties integrating visual and auditory information during prosodic processing due to impairments in temporal syllable integration and speech perception [15]. Given the role of theta band coherence between frontal and posterior regions in learning [21], these connectivity differences likely significantly impact language acquisition.

Continuing with altered causation between central and frontal regions (C4-F7, Fp1-C3). Central areas are involved in sensorimotor functions, while frontal regions support executive operations. fMRI evidence reveals atypical activations during reading in dyslexic children, potentially indicating attempted compensation for phonological processing weaknesses using alternative neural pathways [16]. Since central regions, including Broca's area, are integral for phonological encoding, and theta synchronization facilitates context encoding [21], differences in central-frontal connectivity could signify challenges coordinating sensory perception and motor output during speech production.

Regarding the gamma band, research has associated oscillations with integrating distributed neural information to facilitate perception, memory, and cognition [11]. Differences in gamma connectivity are observed between occipital and parietal (O2-P4), occipital and temporal (O1-T7) areas in people with dyslexia, as it is reflected in Figure 6 and Figure 7. As occipital regions mediate visual processing while temporal/parietal areas support speech and language integration, altered cross-talk between these domains aligns with theories that multi-sensory deficits in dyslexia stem from atypical interplay between vision and language functions [2]. Given gamma's role in binding neural networks through synchronized firing patterns, dyslexic connectivity differences likely signify less efficient audio-visual integration, which may complicate prosodic processing.

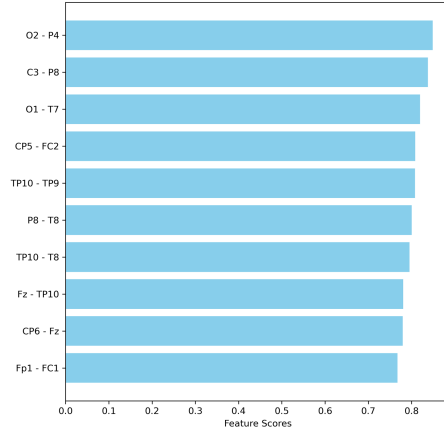


Fig. 6: Bar graph of FS, gamma

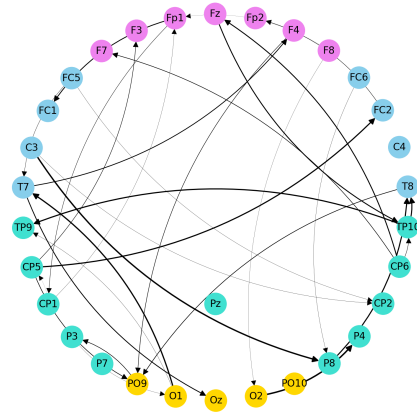


Fig. 7: Connectogram of FS, gamma

Furthermore, central-temporal/parietal gamma (O1-T7, C3-P8) alterations indicate problems coordinating auditory perception and articulatory movements for fluent reading. This theory is based on the importance of aligning sensorimotor and sensory activity (CP5-Fc2) for skilled reading [22]. Rearranged dependencies between visual, speech-motor, and language regions are proposed to precipitate phonological deficits in DD. As gamma oscillations enable neural computations underlying comprehension [20], atypical connections between these areas may constitute network inefficiencies.

Table 1: Results of GB classifier

Band	Accuracy	AUC
Delta	0.855	0.857
Theta	0.896	0.929
Alpha	0.856	0.891
Beta	0.861	0.879
Gamma	0.865	0.911

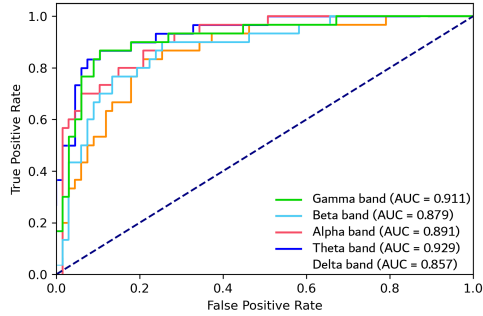


Fig. 8: ROC curves

From Table 1 and ROC curves of Figure 8, we can infer classification analysis that implicates theta and gamma bands in phonological weaknesses in the DD group due to rhythm processing inefficiencies in auditory areas[6]. Consequently, observing connectivity patterns in these bands offers insights into dyslexics' atypical sensorimotor and cognitive coordination. Manipulating theta oscillations to study impacts on speech processing[10] further demonstrates the importance of this frequency range for language and its disorders. Analyzing dyslexics' theta and gamma connectivity dynamics provides perspectives on multisensory, sensorimotor, and temporal integration deficits.

4 Conclusions

By representing directional connectivity strengths between EEG channels, the methodology reveals network integration deficiencies in people with dyslexia within theta and gamma bands during foundational auditory processing. The automated pipeline integrating signaling processing, mapping, feature selection, and classification paves the way for innovative diagnostic screens and interventions for neurodevelopmental disorders. Findings provide perspectives on multisensory, sensorimotor, and temporal integration anomalies underlying reading and oral language difficulties in dyslexia.

Acknowledgments

This work was supported by projects PID2022-137461NB-C32, PID2022-137629OA-I00 and PID2022-137451OB-I00 (Ministerio de Ciencia, Innovación y Universidades), UMA20-FEDERJA-086 (Consejería de Economía y Conocimiento, Junta de Andalucía) and by European Regional Development Funds (ERDF), BioSiP(TIC-251) group and University of Málaga (UMA). M.A.F. grant PRE2019-087350 funded by MCIN/AEI/10.13039/501100011033 by “ESF Investing in your future”, I.R.-R. funded by Plan Andaluz de Investigación, Desarrollo e Innovación (PAIDI), Junta de Andalucía.

References

1. Akaike, H.: A new look at the statistical model identification. *IEEE transactions on automatic control* **19**(6), 716–723 (1974). https://doi.org/10.1007/978-1-4612-1694-0_16
2. Artoni, F., d’Orio, P., Catricalà, E., Conca, F., Bottoni, F., Pelliccia, V., Sartori, I., Russo, G.L., Cappa, S.F., Micera, S., et al.: High gamma response tracks different syntactic structures in homophonous phrases. *Scientific reports* **10**(1), 7537 (2020). <https://doi.org/10.1038/s41598-020-64375-9>
3. Bullmore, E., Sporns, O.: Complex brain networks: graph theoretical analysis of structural and functional systems. *Nature reviews neuroscience* **10**(3), 186–198 (2009). <https://doi.org/10.1038/nrn2575>
4. González, G.F., Van der Molen, M., Žarić, G., Bonte, M., Tijms, J., Blomert, L., Stam, C., Van der Molen, M.: Graph analysis of eeg resting state functional networks in dyslexic readers. *Clinical Neurophysiology* **127**(9), 3165–3175 (2016). <https://doi.org/10.1016/j.clinph.2016.06.023>
5. Górriz, J., Álvarez-Illán, I., Álvarez-Marquina, A., Arco, J., Atzmueller, M., Ballarini, F., Barakova, E., Bologna, G., Bonomini, P., Castellanos-Dominguez, G., et al.: Computational approaches to explainable artificial intelligence: Advances in theory, applications and trends. *Information Fusion* **100**, 101945 (2023). <https://doi.org/10.1016/j.inffus.2023.101945>
6. Goswami, U.: A temporal sampling framework for developmental dyslexia. *Trends in cognitive sciences* **15**(1), 3–10 (2011). <https://doi.org/10.1016/j.tics.2010.10.001>
7. Granger, C.W.: Investigating causal relations by econometric models and cross-spectral methods. *Econometrica: journal of the Econometric Society* **37**(3), 424–438 (1969). <https://doi.org/10.2307/1912791>
8. Guha, R., Ghosh, K.K., Bhowmik, S., Sarkar, R.: Mutually informed correlation coefficient (micc)-a new filter based feature selection method. In: 2020 IEEE calcutta conference (CALCON), pp. 54–58. IEEE, IEEE (2020). <https://doi.org/10.1109/calcon49167.2020.9106516>

9. Hu, F., Wang, H., Wang, Q., Feng, N., Chen, J., Zhang, T.: Acrophobia quantified by eeg based on cnn incorporating granger causality. *International Journal of Neural Systems* **31**(03), 2050069 (2021). <https://doi.org/10.1088/1741-2552/abcdbd>
10. Marko, M., Cimrová, B., Riečanský, I.: Neural theta oscillations support semantic memory retrieval. *Scientific reports* **9**(1), 17667 (2019). <https://doi.org/10.1038/s41598-019-53813-y>
11. Meeuwissen, E.B., Takashima, A., Fernández, G., Jensen, O.: Evidence for human fronto-central gamma activity during long-term memory encoding of word sequences. *PLoS one* **6**(6), e21356 (2011). <https://doi.org/10.1371/journal.pone.0021356>
12. Molinaro, N., Lizarazu, M., Lallier, M., Bourguignon, M., Carreiras, M.: Out-of-synchrony speech entrainment in developmental dyslexia. *Human brain mapping* **37**(8), 2767–2783 (2016). <https://doi.org/10.1002/hbm.23206>
13. Ortiz, A., Martínez-Murcia, F.J., Luque, J.L., Giménez, A., Morales-Ortega, R., Ortega, J.: Dyslexia diagnosis by eeg temporal and spectral descriptors: An anomaly detection approach. *International Journal of Neural Systems* **30**(07), 2050029 (2020). <https://doi.org/10.1142/s012906572050029x>
14. Peterson, R.L., Pennington, B.F.: Developmental dyslexia. *The lancet* **379**(9830), 1997–2007 (2012). [https://doi.org/10.1016/s0140-6736\(12\)60198-6](https://doi.org/10.1016/s0140-6736(12)60198-6)
15. Poeppel, D., Idsardi, W.J., Van Wassenhove, V.: Speech perception at the interface of neurobiology and linguistics. *Philosophical Transactions of the Royal Society B: Biological Sciences* **363**(1493), 1071–1086 (2008). <https://doi.org/10.1093/oso/9780199561315.003.0011>
16. Pugh, K.R., Mencl, W.E., Jenner, A.R., Katz, L., Frost, S.J., Lee, J.R., Shaywitz, S.E., Shaywitz, B.A.: Functional neuroimaging studies of reading and reading disability (developmental dyslexia). *Mental retardation and developmental disabilities research reviews* **6**(3), 207–213 (2000). [https://doi.org/10.1002/1098-2779\(2000\)6:3;207::aid-mrdd8;3.0.co;2-p](https://doi.org/10.1002/1098-2779(2000)6:3;207::aid-mrdd8;3.0.co;2-p)
17. Rodríguez-Rodríguez, I., Ortiz, A., Gallego-Molina, N.J., Formoso, M., Woo, W.L.: Eeg interchannel causality to identify source/sink phase connectivity patterns in developmental dyslexia. *International Journal of Neural Systems* **33**(04), 2350020 (2023). <https://doi.org/10.1142/s012906572350020x>
18. Romeo, R.R., Segaran, J., Leonard, J.A., Robinson, S.T., West, M.R., Mackey, A.P., Yendiki, A., Rowe, M.L., Gabrieli, J.D.: Language exposure relates to structural neural connectivity in childhood. *Journal of Neuroscience* **38**(36), 7870–7877 (2018). <https://doi.org/10.1523/jneurosci.0484-18.2018>
19. Schmidt, C., Piper, D., Pester, B., Mierau, A., Witte, H.: Tracking the reorganization of module structure in time-varying weighted brain functional connectivity networks. *International journal of neural systems* **28**(04), 1750051 (2018). <https://doi.org/10.1142/s0129065717500514>
20. Spironelli, C., Angrilli, A.: Developmental aspects of language lateralization in delta, theta, alpha and beta eeg bands. *Biological psychology* **85**(2), 258–267 (2010). <https://doi.org/10.1016/j.biopsycho.2010.07.011>
21. Summerfield, C., Mangels, J.A.: Coherent theta-band eeg activity predicts item-context binding during encoding. *Neuroimage* **24**(3), 692–703 (2005). <https://doi.org/10.1016/j.neuroimage.2004.09.012>
22. Wang, L., Zhu, Z., Bastiaansen, M.: Integration or predictability? further specification of the functional role of eeg gamma-band oscillations during language comprehension. *Frontiers in psychology* **3**(187) (2012). <https://doi.org/10.3389/fpsyg.2012.00187>
23. Yaqub, M.A., Hong, K.S., Zafar, A., Kim, C.S.: Control of transcranial direct current stimulation duration by assessing functional connectivity of near-infrared spectroscopy signals. *International Journal of Neural Systems* **32**(01), 2150050 (2022). <https://doi.org/10.3390/bioengineering10070810>